Stopping power and ranges of fast ions in heavy elements

Hans Bichsel
1211 22nd Avenue East, Seattle, Washington 98112-3534
(Received 24 September 1990; revised manuscript received 23 April 1992)

For the calculation of stopping power and ranges with the method suggested by Bethe, functions expressing the binding of the electrons in the atoms ("shell corrections") are needed. Here, shell corrections calculated with hydrogenic wave functions have been employed. By using experimental atomic energy levels as parameters for them, I have found good agreement between experimental and calculated values of stopping power for elements with atomic number $Z > 56$. Only for the mean ionization energy I there was no simple relation to atomic properties, and a considerable dependence of the Bloch parameter $b = I/Z$ on Z has been found. Calculated values of stopping power and ranges agree with experimental values for protons with kinetic energies T above 0.5 MeV, for ions (with z protons and $M \leq 40$ nucleons) above $T/M \sim (z - 1.5)$ MeV, well within the uncertainty of the experiments, but an approximately 1% discrepancy for several hundred MeV protons remains.

PACS number(s): 34.50.Bw, 52.40.Mj

I. INTRODUCTION

Calculations of stopping power S, in the tradition of the Bethe-Bloch method [1–3] including shell corrections and the Barkas effect correction term, agreed well with experimental data for protons and α particles with kinetic energies T/M (M is the number of nucleons in the particle) above 0.5-MeV traversing light elements for which values of the mean ionization-energy I had been determined independently [4]. For heavier elements, experimental I values and scaled shell corrections based on Walske's functions [5, 6] were used to calculate S (e.g., [7–9]). For the heaviest elements (Au and Pb) this approach was not suitable for proton energies below about 3 MeV. Since shell corrections for the M shells [10] and the L subshells [11] are now available, I have extended the algorithm to calculate stopping power to include these functions. Corrections for the outer (N, O, P, and Q) shells were derived from the M-shell corrections with a scaling procedure using experimental atomic energy level data. It is thus possible to calculate S and ranges for all elements with $57 \leq Z \leq 92$, with only the I value a free parameter not simply related to Z. It will be seen that, for most data, the agreement between calculated and experimental values is well within experimental errors. The present study is an outgrowth of earlier work [12–14] and is an effort complementary to those by Andersen and Ziegler [15, 16] and Janni [8]. Many observations about problems with experimental data were made in these references and should be studied there.

II. PROCEDURE

It is not possible to calculate S *a priori* with an accuracy of, say, 1%, and empirical modifications of the theoretical functions are used to get calculated values S_t agreeing with experimental data S_x. Here, it is assumed that a major uncertainty in the calculation of stopping power stems from our knowledge of shell corrections. Parameters used in defining them should have values plausibly related to atomic energy levels, so that it is possible to obtain S for all elements. Relativistic corrections for atomic properties were not used. It is shown in the Appendix that they might improve the method.

A. Stopping power S

The expression used for the calculation of the stopping power of particles, consisting of M nucleons, with charge ze, speed v, and kinetic energy T is

$$S = -\frac{dT}{dx} = k\,\frac{z^2}{A\beta^2}\,ZB \tag{1}$$

with $x = t\rho$ the surface density of the absorber (g/cm^2), ρ its density (g/cm^3), t its thickness (cm), $k = 4\pi e^4 N_0/mc^2 = 4\pi r_0^2 N_0 mc^2 = 0.307\,075$ MeV cm^2, $\zeta = T/M_0c^2$, $\beta = v/c$, $\beta^2 = \zeta(2+\zeta)/(1+\zeta)^2$, $\gamma = 1 + \zeta$, $\gamma^2 = 1/(1-\beta^2)$, e the electron charge, m its rest mass ($mc^2 = 510\,999$ eV), c the speed of light, $r_0 = e^2/mc^2 = 2.817\,941 \times 10^{-13}$ cm the classical electron radius, $N_0 = 6.022\,134 \times 10^{23}$ atoms/mol, (Avogadro's number), Z the atomic number of the absorber, A its atomic weight (in g/mol), and B the stopping number (L in some papers). M_0 the rest mass of the particle (protons: $M_0c^2 = 938.2723$ MeV, α particles: 3727.316 MeV). Either β or T is used as the variable indicating the particle speed. As will be seen, this function is valid for $T \geq 0.5$ MeV for protons, $T/M \geq (z - 1.5)$ MeV for $z \geq 2$.

For particles heavier than electrons, Bethe gave the stopping number B in the form

$$B = \ln\frac{2mc^2\beta^2\gamma^2}{I} - \beta^2 \equiv f(\beta) - \ln I, \tag{2}$$

where I is the mean excitation energy of the absorber. With the inclusion of the correction terms, B is now written as

$$B(z) = B_0 + zL_1 + L_2(z) + [G(z,\beta) - \delta(\beta)]/2 \quad (3)$$

with

$$B_0(\beta) = f(\beta) - \ln I - \frac{C(\beta)}{Z}, \quad (4)$$

where $C(\beta)$ is the total shell correction, $G(z,\beta)$ the Mott correction term, δ the correction for the density effect, L_1 the Barkas correction term, and L_2 the Bloch correction term. For the study of experimental data, it is useful to define the experimental value of the stopping number B_x obtained by solving Eq. (1) for an experimental value S_x of the stopping power:

$$B_x(\beta) = S_x(\beta)\frac{A\beta^2}{kz^2Z} \quad (5)$$

and an "experimental I value" I_x defined by

$$\ln I_x \equiv f(\beta) - B_x(\beta) - \frac{C(\beta)}{Z} + zL_1 + L_2(z) + [G(z,\beta) - \delta(\beta)]/2. \quad (6)$$

The various terms in Eqs. (3) and (4) are considered next.

B. I values

In the present approach, experimental I values were calculated with Eq. (6) for experimental values B_x, and an average experimental value I_e was determined by examining all experimental values. Values $b_e = I_e/Z$ are given in Table I and are discussed in Sec. IV. If the function given in Eqs. (3) and (4) is complete, I_e will agree with the value derived from the complex dielectric function $\epsilon(E,0)$ [3]:

$$\ln I = \frac{2}{\pi(hf)^2}\int_0^\infty E\ \mathrm{Im}\left[\frac{-1}{\epsilon(E,0)}\right]\ln E\ dE, \quad (7)$$

where E is the energy transfer in a collision. $\epsilon(E,0)$ is related to the optical properties of the material (e.g., [17]), and hf is the plasma energy [3], defined by $(hf)^2 = 830.4\rho Z/A$ (hf in eV). The only metals for which I was calculated with Eq. (7) are Al [18] and, partially, Si [19]. For most solids, insufficient information is available about $\mathrm{Im}[-1/\epsilon(E,0)]$ to permit this method of determining I.

For preliminary estimates of I, the Bloch parameter is useful:

$$b \equiv I/Z. \quad (8)$$

Trends of the dependence of b on Z may be evident from three quantities: hf_v, b_L, and hf, given in Table I. hf_v is the most probable energy loss to valence electrons, observed in electron energy-loss spectra [20]; it is a major feature of $\epsilon(E,0)$, depends on the structure of the metal and the number of valence electrons, and thus will not relate simply to Z. $b_L = I_L/Z$ is an I value calculated for *atoms* with the local plasma model [21]; it may indicate the trend of I related to inner shells (see [22], though). The plasmon energy hf replaces the I value in S for very high speeds. The small values of all three quantities for Pb compared to those for Au may explain why the experimental value of the Bloch parameter b_e for Pb is smaller than that for Au. Values used earlier [8, 15, 23] are also given in Table I.

TABLE I. Values of Bloch parameters $b = I/Z$ from various sources, and related quantities (Sec. II B): average experimental plasmon energies hf_v [20] and plasma energies hf all in eV. b_L was calculated for atoms with a local density model [21]. b_e is the average experimental value from Fig. 4. Values used in other tabulations are b_J [8], b_A [15], and b_I [23]. They differ from b_e because different shell corrections and different experimental data sets were used. Note the systematic trends with Z.

Z		hf_v	hf	b_L	b_e	b_J	b_A	b_I
57	La		45.9	8.53	8.32	9.75	8.42	8.8
58	Ce		48.2	8.6	8.76	9.75	8.5	8.8
59	Pr		48.5	8.67	8.64	9.76	8.59	9.1
62	Sm		50.6	9.04	9.05	9.78	8.84	9.78
64	Gd		51.5	9.08	8.83	9.27	8.81	9.2
66	Dy		53.7	9.4	9.17	9.8	9.09	9.8
67	Ho		54.5	9.36	9.55	9.8	9.3	9.8
68	Er		55.6	9.6	9.56	9.11	9.41	9.7
70	Yb		48.3	9.65	9.66	9.82	9.46	9.82
72	Hf		66.2	9.76	9.32	9.83	9.47	9.83
73	Ta		74.6	9.78	10.05	10.11	9.37	9.8
74	W	25	80.3	9.8	10.53	10.17	9.36	9.8
77	Ir		86.5	9.87	10.23	9.93	9.55	9.8
78	Pt	23	84.2	9.96	10.08	10.58	9.73	10.1
79	Au	24	80.2	10	10	10.21	9.56	10
82	Pb	15	61.1	9.79	9.5	9.99	9.26	10
83	Bi	18	56.9	9.71	8.98	9.87	9.22	9.9
90	Th		61.3	9.06	8.51	8.18	9.17	9.4
92	U		77.4	9.16	9.09	9.56	9.21	9.7

C. Shell corrections $C(v, Z)$

1. General

In the approach formulated by Bethe, shell corrections must be calculated on a shell-by-shell basis:

$$C(Z,v) = \sum_\nu C_\nu(Z,v) = C_K(Z,v) + C_L(Z,v) + C_M(Z,v) + \cdots. \quad (9)$$

Usually, the dependence on particle speed is expressed in terms of the variable η:

$$\eta_\nu = (mv^2/2)/(mv_0^2Z_\nu^2/2) \equiv (mv^2/2)/\epsilon_\nu \quad (10)$$

with $\epsilon_\nu = RZ_\nu^2$, v_0 the Bohr speed ($v_0 = c/137$), $R = mv_0^2/2 = 13.6$ eV the Rydberg energy, and Z_ν the effective charge of the absorber atoms for electrons in shell

ν. The dependence of C_ν on the atomic number Z also enters via the ionization energy J_ν, expressed in terms of

$$W_\nu = J_\nu/\epsilon_\nu. \tag{11}$$

In principle [8], these functions should be calculated for each subshell in the atom [24]. Here, a somewhat simpler approach was used, as outlined below.

Shell corrections for K and L shells were derived by Walske [5, 6] with the nonrelativistic hydrogenic approximation. Recently, the corrections for the M shells [10] and the L subshells have been calculated [11], with the same approximation. For the outer shells no calculations have been made, and a scaling procedure was used in which it was assumed that the shell corrections for outer shells have the same shape as those for the inner shells [12, 25]. Vertical V_ν and horizontal H_ν scaling factors were introduced:

$$C_\nu = V_\nu C_\mu(W_\mu, H_\nu \eta_\mu), \tag{12}$$

where ν stands for any one of the outer shells and μ stands for the inner shell. H_ν is expected to be equal to the ratio of ionization energies J_μ/J_ν and V_ν related to the number of electrons in the shell. In order to assess the plausibility of this approach, it is instructive to compare the shapes of the known shell corrections. In Fig. 1, they are shown for K, L, and M electrons in gold. The functions have been plotted in such a way as to coincide at the maximum value. Clearly, the functions are similar in shape, and the scaling procedure can be used with some justification, but some leeway will be needed in the choice of H_ν and V_ν. At present it is not known how closely the hydrogenic calculations approximate the correct functions.

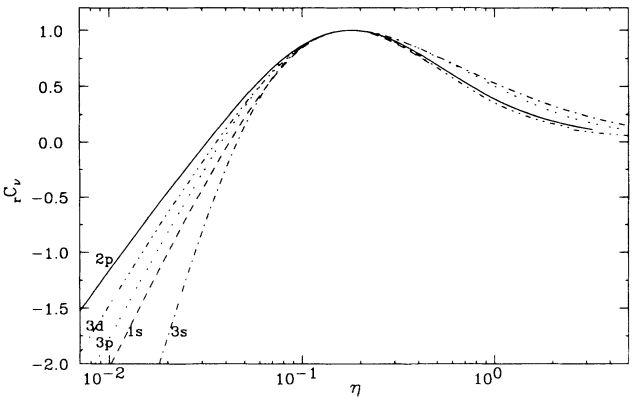

FIG. 1. Shell corrections C_ν calculated for gold with the nonrelativistic hydrogenic approximation [5, 10, 11]. The scaled functions $_rC_\nu$ are plotted vs a common, scaled abscissa η. The scaling was chosen to give the ordinate value 1.0 at the maximum for each function and to have the maximum value at the same value of the abscissa, viz. η =0.18. The actual function C_ν can be obtained by using $\eta_\nu = f_\nu \eta$, and $C_\nu(\eta_\nu) = g_\nu {}_rC_\nu(\eta)$, where f_ν and g_ν are given below.

			W_ν	f_ν	g_ν	n
K	$1s$	– – – – – –	0.876	6.03	1.04	2
L_{II}	$2p$	————	0.182	0.999	1.472	2
M_I	$3s$	– · – · – · – ·	0.081	0.616	0.561	2
M_{II}	$3p$	· · · · · ·	0.072	0.444	1.04	2
M_{IV}	$3d$	– · · – · · – · ·	0.039	0.403	3.524	4

The functions for L_I, L_{III}, M_{III}, and M_V lie within the extremes shown (L_I lies very close to M_I). Note that g_ν is not closely related to the number of electrons n in the subshells, and f_ν is only approximately proportional to $W_\nu = J_\nu/\epsilon_\nu$ (Table II).

TABLE II. Parameters used for the calculation of shell corrections for the L- and M-shells for some heavy elements. n_ν is the number of electrons in each subshell. The total number of electrons included in these shells is 26. In the first line for each element, the value of the energy unit, ϵ_ν, Eq. (10), for each subshell is given in keV. In the second line, the ionization energy is given in these units, $W_m = J_\nu/\epsilon_\nu$, Eq. (11), where J_ν is the measured ionization energy [24].

Element \ Shell	L_I	L_{II}	L_{III}	M_I	M_{II}	M_{III}	M_{IV}	M_V
n_ν	2	2	4	2	2	4	4	6
^{57}La	23.94	37.91	37.91	19.57	19.78	19.78	25.22	25.22
	0.262	0.155	0.145	0.07	0.061	0.057	0.034	0.033
^{64}Gd	30.32	48.48	48.48	25.98	26.51	26.51	34.38	34.38
	0.276	0.164	0.149	0.072	0.064	0.058	0.035	0.034
^{73}Ta	39.55	63.97	63.97	35.5	36.49	36.49	48.05	48.05
	0.295	0.174	0.154	0.076	0.068	0.06	0.037	0.036
^{79}Au	46.34	75.51	75.51	42.29	43.73	43.73	58.36	58.36
	0.31	0.182	0.158	0.081	0.072	0.063	0.039	0.038
^{82}Pb	49.66	81.63	81.63	45.99	47.58	47.58	63.9	63.9
	0.319	0.186	0.16	0.084	0.075	0.064	0.04	0.039
^{92}U	60.21	99.65	99.65	56	58.49	58.49	80.4	80.4
	0.361	0.21	0.172	0.096	0.085	0.071	0.045	0.044

2. Present approximation: K, L, and M shells

The functions mentioned above [5,10,11,26] were used. The effective charge, Z_ν in Eq. (10), was chosen to be $n\zeta$, where n is the principal quantum number and ζ the orbital exponent given by Clementi, Raimondi, and Reinhardt [27]. For the K shell, $Z_K = Z - 0.3$ was used. The quantities ϵ_ν and W_ν for some elements are given in Table II. From the variations in W_ν for the subshells and from the differences in shape seen in Fig. 1 it is evidently advisable to calculate C_ν for each subshell separately.

3. N, O, P, and Q shells

From the values of the scaling factors f_ν and g_ν in Fig. 1 we must expect an uncertainty of ±10 to 20% in the values of H_ν, while for V_ν it might be as much as ±50%. Within these limits they are chosen to give good agreement with experimental data. The ionization energies for the outer shells of some of the heavy elements are given in Table III. In view of the uncertainty of the choice of H_ν, it is reasonable to consider shell correction functions for groups of subshells for which the ionization energies are similar: N_I to N_III; N_IV and N_V; and all the other shells. Note that the number of electrons in N_I to N_V is the same for all $Z \geq 57$. I have named the functions C_{N_1}, C_{N_2}, and C_{N_3}, needing six parameters H_1, V_1, H_2, V_2, H_3, and V_3. Initially it was not clear how many of these parameters should be considered adjustable. Plausibly, H_1 and H_2 are defined by

$$H_\nu = J_{M_\mu} \sum \frac{n_\nu}{J_{N_\nu}} \Big/ \sum n_\nu, \tag{13}$$

where n_ν is the number of electrons in subshell ν (Table III), and V_1 and V_2 might be about 1.3 ± 0.6, and independent of Z. For all electrons outside of N_V (in gold a total of 33 electrons, with ionization energies between 0 and 108 eV) a single function $C_{N_3}(Z,v)$ was used, with H_3 and V_3 as adjustable parameters (H_3 might be $2H_2$ or greater, and V_3 might be expected to depend on Z). Thus four parameters, viz. H_3 and V_ν, must be determined from experimental data (Sec. II F). With this approach, the shell corrections for the outer shells will also compensate for residual errors in L_1, L_2, and z^*.

D. Other corrections

The need for z^3 and z^4 corrections was established experimentally by Andersen *et al.* [28]. Basbas [29] discussed the problem in a general context. Bichsel [30] analyzed experimental data and found that for Au only an empirical function for L_1 approximated experimental data (extending from 1 to 4 MeV) well:

$$L_1(\beta) = 0.002\,833\beta^{-1.2}. \tag{14}$$

The experimental uncertainty of L_1 is less than 10%. The corresponding expression for Ag ($Z = 47$) differs by less than 20%. Thus the use of Eq. (14) for all $Z \geq 57$ seems reasonable. The extrapolation to all proton energies is tentative, but is appropriate for antiprotons in gold to 0.5 MeV [31].

The term L_2 is written in the form derived by Bloch [2]:

$$L_2 = \psi(1) - \mathrm{Re}[\psi(1+iy)] = -y^2 \sum_{j=1}^{\infty} \frac{1}{j(j^2+y^2)}, \tag{15}$$

where ψ is the logarithmic derivative of the Γ function [32], and $y = zv_0/v = z\alpha/\beta$ ($\alpha = 1/137.036$ is the fine-structure constant). For $y^2 \ll 1$, the sum is equal to 1.202....

Bichsel [30] found that it was not necessary to use any charge-state corrections for protons and α particles with $T/M \geq 0.5$ MeV. For Li ions, a reduced charge $z^* < 3$ appears to be needed for $T/M < 2$ MeV, but no definite form of z^* could be derived from the experiments. For lower energies, the need for charge-state corrections will be seen in the figures. Nuclear collisions contribute less than 0.1% to the stopping power at the energies considered here, and thus are neglected. Ahlen [33, 34] gave a close-collision correction $G(z,\beta)$ due to the Mott cross section. It is less than 0.1% of B for protons and α particles, but will be important for heavy ions (e.g., about 2% for 3000-MeV Ca ions, 15% for relativistic U ions)

TABLE III. Ionization energies J_ν [24] and horizontal scaling factors H_1 and H_2 for the calculation, Eq. (12), of the shell corrections C_{N1} (the average value for the 8 electrons in shells N_I to N_III) and C_{N2} (for the ten electrons in shells N_IV and N_V). Values of H_1 and H_2 are defined by the average value of the ratios $J_{M_\mathrm{V}}/J_{N_\nu}$, weighted with number n_ν of electrons in each subshell.

Element \ Shell	M_V	N_I	N_II	N_III	N_IV	N_V		
n_ν	6	2	2	4	4	6		
			J_ν (eV)				H_1	H_2
La	832	270	206	191	99	99	3.96	8.4
Gd	1185	376	289	271	141	141	4	8.4
Er	1409	449	366	320	177	168	3.94	8.22
Ta	1735	566	465	404	241	229	3.84	7.43
Au	2206	759	644	545	352	334	3.6	6.47
Pb	2484	894	764	644	435	413	3.43	5.89
U	3552	1441	1273	1045	780	738	3.01	4.71

and is included in the present algorithm. The function used here for the density effect has been given by Sternheimer, Seltzer, and Berger [35]. The effect amounts to less than 0.04% for 20-MeV protons in gold, and thus is only important for some of the measurements at high energies.

E. Ranges and multiple scattering

Ranges were calculated from stopping power S with the continuous-slowing-down approximation

$$R(T) = R(T_1) + \int_{T_1}^{T} \frac{dT'}{S(T')}. \quad (16)$$

For present purposes, for protons, $T_1 = 0.4$ MeV, and $R(T_1)$ was taken as the total pathlength given by Janni [8]. For 10-MeV protons in Au, this contribution amounts to less than 1% of the total range. Due to multiple scattering, experimental projected ranges are shorter than $R(T)$ [7, 8, 36–39].

F. Method for parameter determination

The parameters to be determined are the I value and the scaling factors H_3 and V_ν of Eq. (12) for the outer-shell corrections. They were found from experimental data with a least-squares-deviation procedure. In earlier studies, the I value was introduced explicitly as a free parameter in the study of the data: the deviation $\delta(\beta) = B(\beta) - B_x(\beta)$ was calculated, and $\sum \delta^2$ was considered as a function of the five parameters. A "best fit" was obtained if the sum was a minimum.

A variation of the parameter I can be avoided if the equation for $\delta(\beta)$ is rearranged as follows [Eq. (6)]:

$$\delta(\beta) + \ln I_a \equiv Y(\beta) \equiv f_m(\beta) - c_i(\beta) - c_o(\beta) + zL_1(\beta) + L_2(\beta) - B_x(\beta), \quad (17)$$

where

$$f_m(\beta) = f(\beta) + [G(z,\beta) - \delta(\beta)]/2, \quad (18)$$

$$c_i(\beta) = \frac{C_K(\beta) + C_L(\beta) + C_M(\beta)}{Z}, \quad (19)$$

$$c_o(\beta) = \frac{C_{N1}(\beta) + C_{N2}(\beta) + C_{N3}(\beta)}{Z}, \quad (20)$$

and I_a is an unknown constant. We define Y_a as the average of p experimental values of $Y(\beta)$:

$$Y_a = \sum Y(\beta)/p, \quad (21)$$

and by assuming $\ln I_a = Y_a$ we get

$$\sum \delta(\beta) = 0. \quad (22)$$

Then, the average deviation σ defined by

$$\sigma^2 = \sum [Y_a - Y(\beta)]^2/(p-1) \quad (23)$$

is the same as $\sum \delta^2/(p-1)$. With this approach, the parameter search is performed for a space reduced by one dimension (i.e., the five-parameter search is reduced to a four-parameter search). σ^2 depends on the parameters and can be considered as a function of the four-dimensional space with coordinates H_3, V_ν. The smallest σ^2 define sets of parameters giving best fits to experimental data.

It was found that there were many local minima of σ^2, and therefore the method of steepest descent was not suitable for the parameter determination; a grid search was used instead. The parameters for small σ^2 were recorded, and the associated functions $Y(\beta)$ were plotted versus particle speed β and examined for systematic deviations. If the deviations $[Y_a - Y(\beta)]$ were randomly distributed, or if they deviated systematically by much less than the experimental error, satisfactory values of the four parameters and the I value

$$I_a = \exp(Y_a) \quad (24)$$

had been found. I_a is subject to systematic errors of S_x and was determined separately for each set of data.

III. EXPERIMENTAL DATA

For most elements, only the experimental data for protons were used for the parameter determination. The data for α particles in Au were used implicitly by the determination of the function L_1 for the Barkas effect [30]. For measurements relative to Al or Cu, tabulated values [7] were used to calculate S_x. Systematic differences occur between experimental data from different sources (see the figures), and the uncertainties σ_e assigned by the authors represent only a qualitative estimate. This means that a simultaneous χ^2 calculation of several data sets is not practical. Therefore, best-fit parameters were determined for each data set, and average values of the parameters were then used. For some data sets where stochastic errors were less than 1% (e.g., [40–43], a smooth function obtained from an independent three-parameter fit (H_3, V_3 and I_a) has been used to represent the data in the figures.

For gold, I designed an average experimental data set for proton energies above 0.3 MeV. Between 0.3 and 1.5 MeV, data by Luomajärvi [44], Semrad [40], Andersen and Nielsen [45], and Santry and Werner [46, 47] were used and given about equal weight. Between 1.5 and 3 MeV, the data by Andersen and Nielsen [45] were reduced by 0.8%. Above 3 MeV, the data by Ishiwari and coworkers [48, 49] and those by Sørensen and Andersen [50] were weighted inversely with their quoted errors. Other data were not used.

For each experimental $S_x(T)$ and calculated $S_t(T)$ value, the relative difference $r(T)$ was determined:

$$r(T) = \frac{S_t(T)}{S_x(T)} - 1. \quad (25)$$

Values of $r(T)$, in percent, are plotted in Figs. 5–8. The average standard deviation σ_x for an experimental data set with p values was defined by

TABLE IV. Symbols used for plotting data in Figs. 3–8.

Reference	Symbol
Oberlin and co-workers [41, 42], Santry and Werner [46, 47]	×
Bader *et al.* [51], Borders [52]	◇
Luomajärvi [44], Langley and Blewer [53]	□
Green, Cooper, and Harris [54]; Knudsen, Andersen, and Martini [55]; Chumanov [56]	✦
Ishiwari and co-workers [48, 49, 57, 58]	⌑
MacKenzie and co-workers [59–62], Lin and co-workers [63, 64]	⌖
Andersen and co-workers [45, 50, 65, 66], Fontell and Luomajärvi [67]	⤫
Semrad [40], Chu *et al.* [68]	⋇
Sirotinin *et al.* [69], Kuldeep and Jain [70]	○

$$\sigma_x^2 = \sum r(T)^2/(p-1). \tag{26}$$

$r(T)$ and σ_x were compared with the errors σ_e of S_x given by the authors. Symbols used in plotting the data in Figs. 2–8 are given in Table IV.

IV. RESULTS OF PARAMETER SEARCHES

From an examination of the experimental data I concluded that only for gold there were enough data to permit a meaningful four-parameter search. Values H_1 and H_2 calculated with Eq. (13) gave better agreement with average experimental data for Au than values different by ±20%, and no further searches were made with different H_1 and H_2. Thus there were now only the four parameters H_3 and V_ν for which values were undetermined. The search showed that $V_1 = 1.25, V_2 = 1.4, H_3 = 13$, and $V_3 = 1.32$ gave a good fit [71]. These values for V_1 and V_2 were used for all elements. For C_{N_1} and C_{N_3}, the function C_{M_V}, for C_{N_2}, $C_{M_{III}}$ was scaled.

It is expected that the parameters H_3 and V_3 associated with electrons in the outermost shells (N_{VI} to Q) will depend on the atomic number Z. Therefore I made a two-parameter search for H_3 and V_3 for all elements. I found that for $Z \geq 73$ the value for gold, $H_3 = 13$, gave satisfactory fits; the values V_3 and I_a varied for each experimental data set. Values of V_3 are plotted in Fig. 2: for the data with the smallest σ_e a tendency toward an increase of V_3 with Z can be discerned. Since V_3 should be related to the number of outermost electrons, $n_0 = Z - 46$, the function

$$V_3 = (Z - 46)/25 \tag{27}$$

was chosen to represent this parameter.

For the elements with $Z \leq 60$, $H_3 = 50$; for $61 \leq Z \leq 72$, $H_3 = 25$ were found to fit experimental data. Then, a one-parameter search was made for V_3. Values giving best fits are shown in Fig. 3. No systematic trend of V_3 with Z can be seen below or above $Z = 60$, therefore I chose constant values, approximately equal to the average for all data, viz. $V_3 = 3.85$ for $Z < 60, V_3 = 2.3$ for $Z \geq 60$.

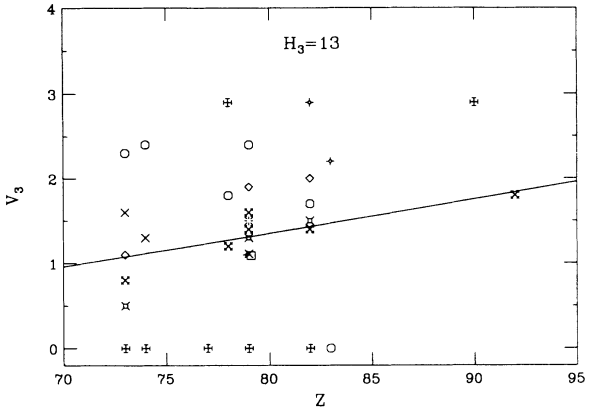

FIG. 2. Values of the vertical scaling factor V_3 for the outermost shells (beyond N_V) for best fits to different experimental data sets for protons, as a function of atomic number Z for $Z \geq 73$. The parameters V_1 =1.25, V_2=1.4, and H_3 =13 were used for all Z. Resulting I values differ for each set (Fig. 4). The function $V_3 = (Z - 46)/25$ is shown as a solid line. It is not possible to assign uncertainties derived from σ_e to individual values because V_3 as well as I would change with changes in S_x. Symbols are related to the references cited in Table IV.

Finally, the average value I_a for each data set was determined with the parameters defined above and the values $b_a = I_a/Z$ are shown in Fig. 4. The σ_x are less than σ_e for most data sets. The fluctuations in I_a seen in Fig. 4 for each Z evidently are in part an expression of the systematic differences between experimental data, but because the values were obtained from data at different energy ranges, they may also indicate possible problems in the functions included in B. Because I, by

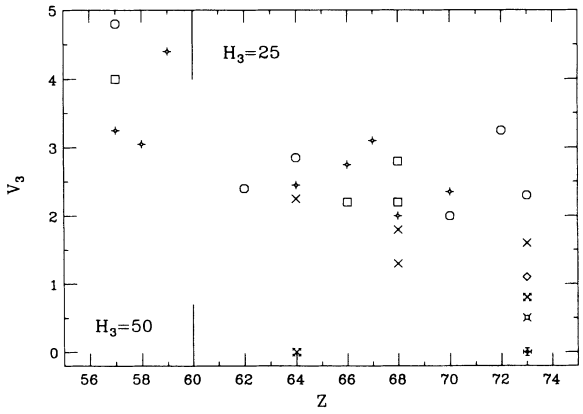

FIG. 3. Same as Fig. 2 for $Z \leq 72$. The following parameters were used: V_1 =1.25, V_2 =1.4 for all Z; H_3 =50 for $Z \leq 60$; H_3 =25 for $Z > 60$. Resulting I values differ for each set of experimental data (Fig. 4). No systematic dependence of V_3 on Z is evident, thus V_3 =3.85 was chosen as an approximate average for $Z < 60$, V_3 =2.3 for $Z \geq 60$. For comparison, the data for Ta (Z =73, H_3 =13) are also shown.

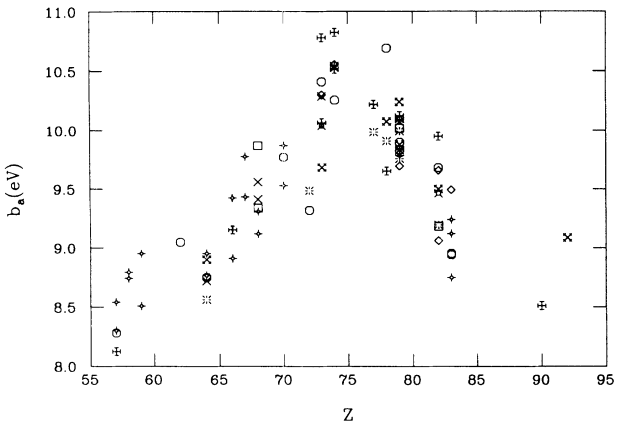

FIG. 4. Values of the Bloch parameter $b_a = I_a/Z$ for different experimental data sets for protons and α particles (symbols from Table IV) as a function of atomic number Z. V_1 =1.25, V_2 =1.4 for all Z; other parameters: for $Z < 60$, $H_3 = 50$, $V_3 = 3.85$; for $60 < Z \leq 72$, $H_3 = 25$, $V_3 = 2.3$; and for $Z > 72$, $H_3 = 13$, $V_3 = (Z - 46)/25$. The different values b_a at each Z express the systematic differences in the experimental data. An uncertainty of $\pm 1\%$ in S_x gives an uncertainty of about $\pm 1\%$ in b_a at 1 MeV, about $\pm 3\%$ at 10 MeV (Table V). The unweighted mean value for $p = 18$ measurements in gold is $I = (788 \pm 12)$ eV; for Pb, $p = 8$, $I = (779 \pm 25)$ eV.

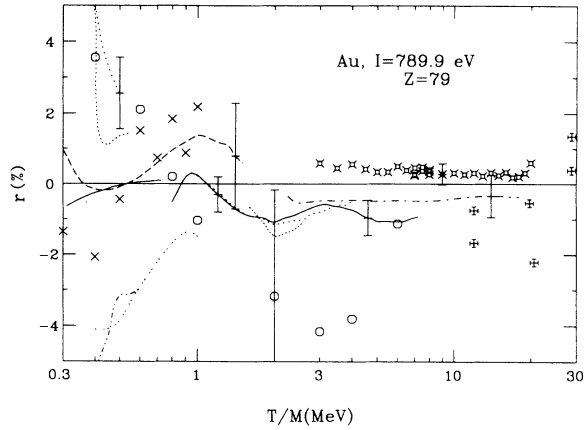

FIG. 5. Comparison of experimental and calculated values of the proton and deuteron stopping power for gold. The relative difference $r(T)$ [Eq. (25)] is given as a function of the kinetic energy per nucleon T/M of the particles. Calculated values were obtained with $V_1 = 1.25$, $V_2 = 1.4$, $H_3 = 13$, $V_3 = (Z - 46)/25 = 1.32$, and $I_e = 789.9$ eV. Symbols are given in Table IV; continuous lines are used for smoothed data; dashed-double dotted, [51]; double-dotted; [54]; dashed, [44]; dash-dotted, [50]; solid line above 0.8 MeV, [45]; below 0.7 MeV, smoothed data by Semrad [40]. The α-particle and Li data of Ref. [28] between 1 and 4 MeV/M are shown by the dotted lines, as are those from [43, 67] below 0.5 MeV. The data from [51, 54] were not included in the data adjustment of Sec. III, thus their deviation is relatively large. Experimental uncertainties σ_e, given by the authors, are shown for only a few values. Negative values of $r(T)$ imply values of I_x less than I_e.

the definition of Eq. (7), is a property of the material, we must use an average of all I_a [Eq. (24)]. The values I have selected are shown in Table I. They are only valid in the context of the other parameters used here, and still depend on the experimental data. An uncertainty of I_e of $\pm 1.5\%$ to $\pm 5\%$ should be assumed. Fluctuations in b_e for neighboring Z may be indicative of systematic errors in the measurements. On the other hand, the trend with Z seen in Fig. 4 is substantial and more pronounced than shown so far (compare to b_J and b_A in Table I). It is notable that b_e and the value b_L calculated with the local density model differ on the average by only $(0.7 \pm 3.6)\%$, even though b_L was calculated for single atoms, while b_e was measured for the metal. On the other hand, there are large changes with Z of the ratio hf/b_e.

V. COMPARISON OF CALCULATED AND EXPERIMENTAL VALUES

A. Protons

The comparison between selected experimental data S_x and calculated functions S_t for $T < 30$ MeV is made in Figs. 5–8. The relative difference $r(T)$, Eq. (25), is shown as a function of reduced kinetic energy T/M of the particles. The authors' experimental uncertainties are shown at only a few energies. Similar functions for Ce, Pr, Sm, Gd, Dy, Ho, Yb, Hf, Ir, Pt, Bi, and U may be found in [71]. There is no evidence to invalidate the adopted function S. It is notable that it agrees with experiments at energies T well below 1 MeV. There are no

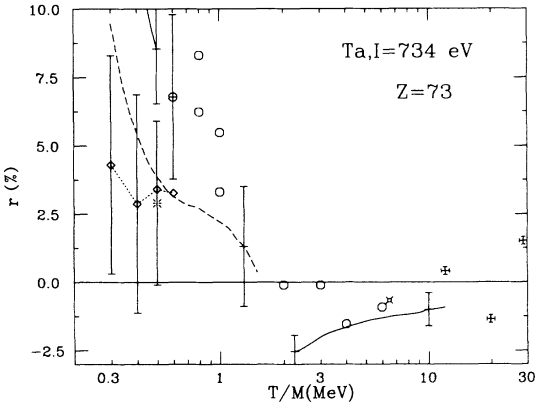

FIG. 6. Same as Fig. 5, for Ta. Calculated values were obtained with $H_3 = 13$, $V_3 = 1.08$, and $I_e = 734$ eV. Continuous lines show data smoothed by the authors, proton data from [51] below 0.6 MeV are shown as the dotted line, and those from [50] above 2.25 MeV as a solid line. The dashed line shows the proton data from [44]. α-particle data from [63] are shown by the solid line ending at 8.5%. The difference in $r(T)$ between the data from [44] and [50] at neighboring energies (1.5 and 2.25 MeV) is about 3%, thus equal to the sum of the experimental errors σ_e. It is unlikely that this is a problem in the algorithm for S.

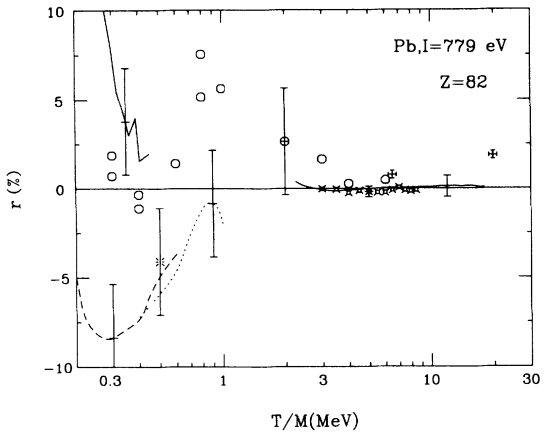

FIG. 7. Same as Fig. 5, for lead, with $H_3 = 13$, $V_3 = 1.44$, and $I_e = 779$ eV. Values of $r(T)$ for the data from [51] (dashed line) and [54] (dotted line) show similar deviation as those for gold. The proton data from [50] and the α-particle data from [52] for $0.3 < T/M$ (MeV) < 0.45 are shown by solid lines.

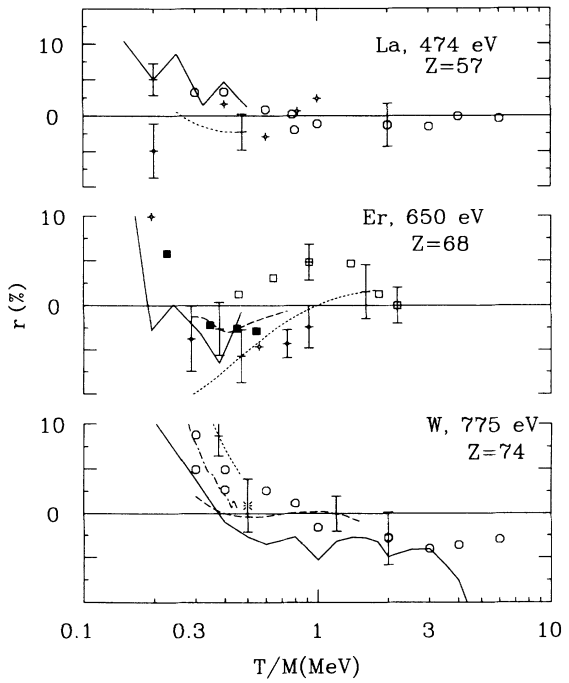

FIG. 8. Same as Fig. 5, for La ($H_3 = 50$, $V_3 = 3.85$), Er ($H_3 = 25$, $V_3 = 2.3$), and W ($H_3 = 13$, $V_3 = 1.12$). The I values $I_e = b_e Z$ (Table I) are shown next to the chemical symbol. For La and Er, the solid lines represent the α data from [55], the dotted line for La those from [63]. For Er, data from [42] are shown as smooth lines which were obtained by making a three parameter fit (H_3, V_3, I_a) to their experimental data: protons, dotted line; α, dashed line. Data for Er from [53] are shown by the squares: open for protons, solid for α. For W, the dotted line represents the α data from [63], the dash-dotted line those from [52], the dashed line the proton data from [44], and the solid line those from [56]. For 2-MeV α, the value from [68] is plotted as a star at 0.5 MeV.

general trends for $r(T)$ to be definitely larger than 0, thus no need for $z^* < 1$ is evident. For Ta, Fig. 6, the agreement between different experiments is poor, but while the data by Luomajärvi [44] differ considerably from S_t, they agree quite well for W and Au. Experimental data for protons with energies between 12 and 73 MeV [59–61, 72] in general agree well with calculated values [71]. For measurements with high-energy protons reported by Bakker and Segrè [73], Barkas and von Friesen [74], Vasilevsky and Prokoshkin [75], and Vasilevsky *et al.* [76], a higher I value (which would reduce S_t) is indicated for Pb and U: further correction terms to the algorithm may be needed (see Appendix).

B. Helium and heavier ions

Selected data for α are shown in Figs. 5–8. The values of $r(T)$ generally increase with decreasing $T/M < 0.5$ MeV, indicating the need for a charge-state correction. Experimental data by Ishiwari *et al.* [77–79] and data by Takahashi *et al.* [80] for α particles and C ions agree with calculated values. For the C ions, L_1 and L_2 amount to 8% and 5% of L, respectively. The expression given by Eq. (14) thus seems to be valid. The Mott term amounts to less than 0.2%. The data for ^{16}O, ^{36}Ar, ^{40}Ar, and ^{40}Ca ions traversing Ta and Au by Bimbot *et al.* [81,82], Gauvin and Hubert [83], and Schwab *et al.* [84] agree well with calculated values [71], except for O ions with

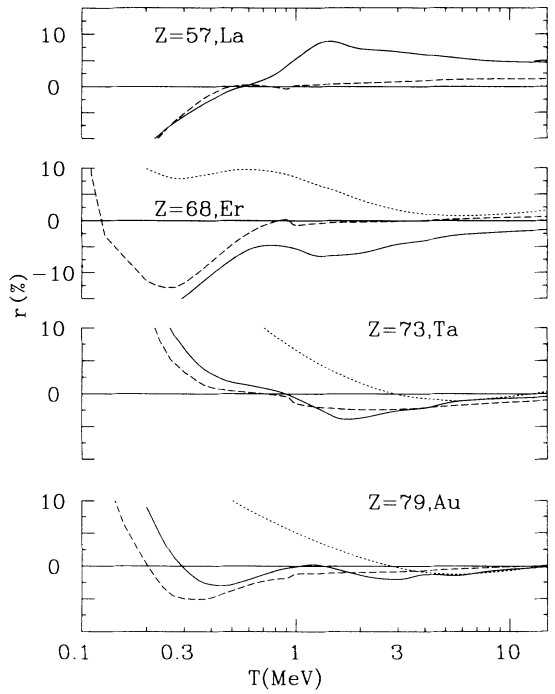

FIG. 9. Comparison between present calculations and some other tabulations. The relative difference $r(T)$ is plotted as a function of proton energy T for four elements. The solid lines represent the functions given by Janni [8], the dotted lines those by Andersen and Ziegler [15], the dashed lines those of Williamson, Boujot, and Picard [89].

TABLE V. Contributions to the stopping number B, Eqs. (3) and (4), for protons of energy T (MeV) passing through a gold absorber with $\ln I = 6.672$. $B_B = f_m(\beta) - \ln I$, Eq. (18). The shell corrections c_i and c_o are defined in Eqs. (19) and (20), L_1 in Eq. (14), and L_2 in Eq. (15). H_1=3.6, V_1=1.25, H_2=6.47, V_2=1.4, H_3=13, V_3=1.32. Note that a fractional change of x% in B (or S) causes a change of (xB)% in the I value.

T	B	B_B	$f_m(\beta)$	c_i	c_o	L_1	$-L_2$
0.30	0.5374	-0.1901	6.4819	−0.6270	0.0398	0.2338	0.0935
0.40	0.6374	0.0974	6.7695	−0.5398	0.1252	0.1968	0.0713
0.50	0.7273	0.3204	6.9924	−0.4724	0.1800	0.1721	0.0577
0.60	0.8097	0.5026	7.1746	−0.4175	0.2163	0.1543	0.0484
0.70	0.8862	0.6565	7.3286	−0.3714	0.2408	0.1407	0.0417
0.80	0.9575	0.7899	7.4619	−0.3317	0.2573	0.1299	0.0366
0.90	1.0245	0.9075	7.5796	−0.2969	0.2683	0.1210	0.0326
1.00	1.0876	1.0127	7.6848	−0.2662	0.2755	0.1136	0.0295
1.10	1.1472	1.1079	7.7799	−0.2386	0.2798	0.1073	0.0268
1.20	1.2037	1.1947	7.8667	−0.2138	0.2820	0.1019	0.0246
1.30	1.2574	1.2746	7.9466	−0.1912	0.2828	0.0971	0.0228
1.40	1.3083	1.3485	8.0206	−0.1703	0.2823	0.0929	0.0212
1.50	1.3573	1.4174	8.0894	−0.1515	0.2809	0.0891	0.0198
1.60	1.4041	1.4817	8.1538	−0.1341	0.2790	0.0857	0.0186
1.70	1.4489	1.5422	8.2142	−0.1180	0.2765	0.0827	0.0175
1.80	1.4920	1.5992	8.2712	−0.1031	0.2736	0.0799	0.0165
1.90	1.5334	1.6531	8.3251	−0.0891	0.2705	0.0774	0.0157
2.00	1.5732	1.7042	8.3763	−0.0761	0.2672	0.0750	0.0149
2.50	1.7533	1.9265	8.5986	−0.0221	0.2491	0.0657	0.0120
3.00	1.9080	2.1080	8.7801	0.0181	0.2309	0.0589	0.0100
3.50	2.0437	2.2614	8.9334	0.0490	0.2137	0.0537	0.0086
4.00	2.1648	2.3941	9.0661	0.0733	0.1981	0.0496	0.0075
5.00	2.3737	2.6156	9.2876	0.1081	0.1712	0.0434	0.0060
10.00	3.0631	3.3007	9.9727	0.1677	0.0956	0.0288	0.0030
30.00	4.2076	4.3686	11.0407	0.1441	0.0310	0.0152	0.0010
100.00	5.4012	5.4819	12.1539	0.0787	0.0095	0.0078	0.0003

$T/M < 6.5$ MeV in Au, where a charge-state correction appears to be necessary. So far, the data are not sufficient to arrive at a quantitative description of $z^*(\beta)$.

C. Range measurements

The ranges of protons in Au measured by Bichsel, Mozley, and Aron [85], corrected by the multiple scattering corrections [36], agree with calculated values, Eq. (16), to ±0.2%. Asymmetries in the range-straggling function [39, 86] have not been taken into account yet. The ranges for protons in lead measured by Bloembergen and van Heerden [87], Mather and Segrè [88], Vasilevsky and Prokoshkin [75] in general exceed calculated ranges by 1–2 %, suggesting a larger I value for Pb, or the need for the correction discussed in the Appendix.

VI. TABLES OF STOPPING POWER

The expression for the stopping number B contains several terms which change quite rapidly at small particle speeds. This can be seen in Table V, where the terms of Eqs. (3) and (4) are shown for protons in gold. The shell corrections are combined into inner shells c_i and outer shells c_o [Eqs. (19) and (20)]. The Bethe approximation is defined by $B_B = f_m(\beta) - \ln I$. For $T > 1$ MeV, B_B differs by no more than 10% from B, but the sum of the corrections still amounts to 1.5% at 100 MeV. With decreasing energy, the various correction terms begin to contribute increasing amounts to B. Around 1 MeV, the net contribution from the shell corrections $c_i + c_o$ is almost zero. All the terms in Eqs. (3) and (4) have a well-defined physical meaning even at the smallest energies listed here, and therefore, no definite energy can be given at which the algorithm is invalid. Measurements with antiprotons in gold show a deviation of L_1 of Eq. (14) at energies below 0.5 MeV [31].

Values of stopping power for p and α calculated with the parameters in Tables II and III, and in Sec. IV are given in Tables VI and VII. They are compared with other tabulations in Fig. 9. Andersen and Ziegler [15] published an evaluation of experimental stopping-power data for protons. For energies greater than 1 MeV, they used five free parameters to calculate the shell corrections. Janni [8] gave stopping powers for protons. He used the scaling procedure of Eq. (12) to obtain shell corrections for each subshell from L-shell corrections [6]. Data from the tables by Williamson, Boujot, and Picard

[89] are also shown. A major reason for the relatively large differences below 2 MeV is the inclusion in the present study of data which were not available for the earlier evaluations [44, 55, 69]. Data for p in Pb above 1 MeV in [7] differ by less than 1% from present values.

VII. CONCLUSIONS

With the functions, scaling factors, and I values given above, good to excellent agreement between calculated and experimental values of stopping power has been obtained. For gold, I estimate the uncertainty (1σ level) of calculated values to be ±2% between 0.5 and 1 MeV, ±1% between 1 and 3 MeV, ±0.5% between 3 and 20 MeV, ±1% above 20 MeV, and ±2% above 100 MeV. For other elements, it may be (±2–4)% below 3 MeV, ±(1–2)% above. The influence of the uncertainty of the I value must be added. The present approach is plausible insofar as it includes all of the elements of current thoughts about the Bethe-Bloch approach. In examining

TABLE VI. Stopping-power table for protons in several elements as a function of kinetic energy T. Below 1 MeV, the uncertainty is several percent; above 1 MeV it is mainly determined by the error in the I value. If a linear interpolation is made for $\ln S$ and $\ln T$, the maximum error of interpolated values is 0.1%.

Element	La	Sm	Er	Ta	Au	Pb	U
A (g/mol)	6.189	7.49	9.15	16.6	19.32	11.36	19.07
I (eV)	474	561	650	734	790	779	841
	Stopping power (MeV cm^2/g)						
T (MeV)	La	Sm	Er	Ta	Au	Pb	U
0.3	153.79	125.71	106.25	117.29	103.41	103.79	87.94
0.4	136.93	113.95	98.23	101.95	92.02	92.59	81.73
0.5	123.67	105.23	92.06	91.86	84.03	84.52	76.13
0.6	113.16	98.12	86.82	84.52	77.99	78.35	71.40
0.7	104.68	92.15	82.24	78.82	73.18	73.43	67.40
0.8	97.707	87.009	78.179	74.208	69.203	69.360	63.976
0.9	91.875	82.533	74.553	70.333	65.830	65.905	61.009
1.0	86.986	78.624	71.307	67.016	62.910	62.920	58.398
1.2	78.882	72.045	65.735	61.534	58.046	57.961	53.998
1.4	72.543	66.719	61.136	57.174	54.097	53.959	50.409
1.6	67.401	62.304	57.262	53.563	50.820	50.628	47.393
1.8	63.113	58.567	53.949	50.499	48.019	47.798	44.811
2.0	59.470	55.344	51.083	47.861	45.586	45.347	42.561
2.5	52.303	48.957	45.324	42.574	40.677	40.409	38.018
3.0	46.964	44.123	40.965	38.557	36.920	36.641	34.524
3.5	42.793	40.317	37.509	35.374	33.926	33.644	31.733
4.0	39.419	37.222	34.688	32.770	31.470	31.191	29.440
4.5	36.620	34.643	32.334	30.590	29.409	29.135	27.517
5.0	34.254	32.456	30.332	28.734	27.650	27.382	25.874
6.0	30.451	28.927	27.094	25.720	24.791	24.538	23.206
7.0	27.512	26.191	24.575	23.371	22.553	22.316	21.119
8.0	25.160	23.994	22.549	21.475	20.744	20.521	19.435
9.0	23.229	22.185	20.877	19.906	19.249	19.038	18.040
10.0	21.609	20.666	19.470	18.585	17.985	17.787	16.863
12.0	19.038	18.247	17.224	16.470	15.960	15.781	14.978
14.0	17.070	16.393	15.503	14.845	14.400	14.239	13.527
16.0	15.527	14.931	14.135	13.551	13.157	13.009	12.370
18.0	14.266	13.736	13.019	12.494	12.140	12.003	11.422
20.0	13.218	12.742	12.089	11.611	11.289	11.162	10.629
25.0	11.232	10.851	10.317	9.926	9.664	9.555	9.112
30.0	9.823	9.506	9.052	8.719	8.498	8.403	8.023
35.0	8.767	8.495	8.099	7.811	7.618	7.533	7.199
40.0	7.943	7.705	7.354	7.098	6.927	6.851	6.552
50.0	6.737	6.546	6.258	6.048	5.909	5.843	5.595
60.0	5.893	5.732	5.487	5.309	5.190	5.133	4.919
70.0	5.267	5.129	4.913	4.757	4.654	4.603	4.415
80.0	4.783	4.661	4.469	4.330	4.237	4.191	4.022
90.0	4.397	4.288	4.114	3.988	3.904	3.862	3.707
100.0	4.082	3.983	3.823	3.708	3.631	3.592	3.450

the data for individual experiments for various Z in Figs. 2–4 it is seen that a single experimental data set cannot be expected to provide the parameters H_3, V_3, and I_a suitable for other data, and it is inadvisable to determine parameters on the basis of a single data set, especially if it extends over a restricted energy range (e.g., [9, 12–14]). If the procedure is to be used for elements not listed in Table I, all parameters are defined above, only an I value must be chosen. This could be done, e.g., by using b_e from a neighboring element or by interpolation using calculated values of b_L.

Many systematic errors of unknown magnitude are associated with the functions used. Examples are (1) use of nonrelativistic hydrogenic wave functions (see Appendix), (2) use of scaling procedure for the calculation of the shell corrections, (3) extrapolation of empirical L_1 to different Z, (4) influence of the approximations used by Bloch in his derivation of L_2, (5) neglect of higher terms in the Born approximation, (6) approximations used for the Mott term and the density effect, (7) neglect of charge exchange effects (e.g., [90]). Most of these errors influence S at the level of $\pm 1\%$ or less. Further developments needed to reduce them appear to be very tedious and may not be worthwhile.

Systematic errors of the experimental data cannot necessarily be discerned. An example is the modification of the Andersen *et al.* [28] data for Au by Andersen and Nielsen [45]. The results for Ta (Fig. 6) do not inspire much trust in the experiments. The results for I_e (Table I) based on a single set of data must be considered to be tentative. I would be surprised if new measurements would show the need for changes in the basic parameters of Tables II and III, and in V_1 and V_2. Measurements for proton energies between 0.5 and 6 MeV for several ele-

TABLE VII. Stopping-power table for α in several elements as a function of kinetic energy T. Below 2.5 MeV, the uncertainty is several percent; above 2.5 MeV it is mainly determined by the error in the I value. If a linear interpolation is made for $\ln S$ and $\ln T$, the maximum error of interpolated values is 0.1%.

Element	La	Sm	Er	Ta	Au	Pb	U
A (g/mol)	138.91	150.35	167.26	180.95	196.97	207.19	238.03
I (eV)	474	561	650	734	790	779	841
	Stopping power (MeV cm^2/g)						
T (MeV)	La	Sm	Er	Ta	Au	Pb	U
1.6	557.42	466.11	403.39	417.59	378.14	380.28	336.91
1.8	529.22	447.58	390.41	395.65	360.96	362.94	325.26
2.0	504.17	431.01	378.50	377.19	346.04	347.86	314.30
2.2	481.71	415.85	367.34	361.23	332.94	334.50	304.16
2.4	461.56	401.92	356.82	347.31	321.29	322.61	294.75
2.6	443.45	389.14	347.00	334.94	310.79	311.91	286.05
2.8	426.94	377.24	337.71	323.83	301.32	302.18	278.01
3.0	412.05	366.17	328.92	313.78	292.66	293.32	270.53
3.5	379.91	341.71	309.11	292.28	273.87	274.12	254.02
4.0	354.18	321.03	291.82	274.59	258.22	258.15	239.99
4.5	332.27	303.20	276.65	259.61	244.87	244.54	227.89
5.0	313.65	287.68	263.31	246.71	233.25	232.76	217.30
5.5	297.56	274.03	251.42	235.45	223.03	222.38	207.95
6.0	283.46	261.91	240.77	225.47	213.92	213.14	199.58
7.0	259.86	241.32	222.50	208.47	198.35	197.43	185.21
8.0	240.73	224.35	207.34	194.48	185.41	184.40	173.22
10.0	211.29	198.01	183.51	172.54	164.98	163.87	154.28
12.0	189.43	178.15	165.55	155.95	149.42	148.28	139.79
14.0	172.39	162.56	151.36	142.85	137.08	135.93	128.27
16.0	158.64	149.92	139.81	132.17	126.99	125.85	118.84
18.0	147.26	139.40	130.20	123.25	118.55	117.43	110.96
20.0	137.65	130.50	122.04	115.67	111.35	110.27	104.24
25.0	118.98	113.15	106.08	100.80	97.22	96.22	91.04
30.0	105.34	100.42	94.34	89.82	86.74	85.82	81.27
35.0	94.861	90.606	85.267	81.309	78.627	77.760	73.698
40.0	86.519	82.775	78.010	74.487	72.101	71.304	67.616
50.0	74.003	70.986	67.059	64.164	62.208	61.510	58.407
60.0	65.007	62.456	59.133	56.670	55.009	54.388	51.705
70.0	58.181	56.018	53.088	50.947	49.501	48.944	46.574
80.0	52.806	50.914	48.316	46.412	45.135	44.625	42.501
90.0	48.453	46.772	44.424	42.722	41.575	41.106	39.180
100.0	44.849	43.336	41.211	39.656	38.611	38.176	36.411

ments with an uncertainty of no more than 0.3% would demonstrate the Z dependence of H_3 and V_3 more clearly. Similar measurements would be required to establish values of H_3, V_3, and I for compounds. An independent determination of I values from Eq. (7) with an uncertainty of less than $\pm 2\%$ is desirable (it would help, e.g., with the problems with the data for Ta). Such I values would also help in establishing the errors of the scaling factors H_ν and V_ν [4].

While approximations better than the nonrelativistic hydrogenic calculations for K-, L-, and M-shell excitations have been made for collision cross sections (e.g., [91–93], these calculations still differ by large amounts from experimental data at low particle speeds. It is thus an open question whether corresponding calculations for the shell corrections would be helpful.

ACKNOWLEDGMENTS

I am grateful to be able to use the computer facilities of the Nuclear Physics Laboratory at the University of Washington and for support by the Greenwalt family trust.

APPENDIX: RELATIVISTIC EFFECTS IN ABSORBER ATOM

Leung [94] described a correction to the Bethe theory which he obtained from considering relativistic effects for the atomic electrons. For Au, he estimated an increase of S of about 2% due to this effect. The change was related to relativistic corrections to the Bethe sum rule [95]. The introduction of this correction term into the present study of the data [with the expression given in Leung's Eqs. (13) and (14)] changes the coefficients H and V for outer-shell electrons, and decreases the I values. For an average data set for Pb, consisting of the data of Ishiwari *et al.* [48, 49] and Sørensen and Andersen [50], the following three-parameter best fit was obtained: $H_3 = 12$, $V_3 = 2$, and $I = 720$ eV, with $\sigma_x = \pm 0.08\%$. The fit is as good as that shown in Fig. 7. If these parameter values are used for all the high-energy data for Pb, the average value of r is $(0.2 \pm 0.9)\%$, compared to $(1.4 \pm 0.9)\%$ for the parameters in Sec. IV. Thus the Leung correction to the stopping-power function brings the calculation into closer agreement with experiment at the higher energies, and it appears desirable to explore this effect in more accurate studies. Also, more accurate measurements at both low and high energies would be useful to assess the accuracy of this correction.

[1] H. Bethe, Ann. Phys. (5. Folge) **5**, 325 (1930).
[2] F. Bloch, Ann. Phys. (5. Folge) **16**, 285 (1933).
[3] U. Fano, Annu. Rev. Nucl. Sci. **13**, 1 (1963).
[4] H. Bichsel and L. E. Porter, Phys. Rev. A **25**, 2499 (1982).
[5] M. C. Walske, Phys. Rev. **88**, 1283 (1952).
[6] M. C. Walske, Phys. Rev. **101**, 940 (1956).
[7] H. Bichsel, in *American Institute of Physics Handbook*, 3rd ed., edited by D. E. Gray (McGraw-Hill, New York, 1972), Chap. 8.
[8] J. F. Janni, At. Data Nucl. Data Tables **27**, 147 (1982).
[9] L. E. Porter and S. R. Bryan, Radiat. Res. **97**, 25 (1984); Nucl. Instrum. Methods **178**, 227 (1980).
[10] H. Bichsel, Phys. Rev. A **28**, 1147 (1983).
[11] H. Bichsel, University of California Radiation Laboratory, Report No. UCRL-17538 (unpublished).
[12] H. Bichsel, University of Southern California Technical Report No. 3, 1961 (unpublished).
[13] H. Bichsel, in *Studies in Penetration of Charged Particles in Matter*, Natl. Acad. Sci. — Natl. Res. Council Publication 1133, 1964, p. 17.
[14] H. Bichsel University of California Radiation Laboratory, Report No. UCRL-17538 (unpublished).
[15] H. H. Andersen and J. F. Ziegler, *Hydrogen Stopping Powers and Ranges in All Elements* (Pergamon, New York, 1977).
[16] J. F. Ziegler, *Helium Stopping Powers and Ranges for All Elemental Matter* (Pergamon, New York, 1977). In Table 1, (p. 55) of this reference the values of S_e for $Z > 72$ and for $10 < T/\text{MeV} \leq 30$ are too small by up to 15%.
[17] J. H. Barkyoumb and D. Y. Smith, Phys. Rev. A **41**, 4863 (1990).
[18] E. Shiles, T. Sasaki, M. Inokuti, and D. Y. Smith, Phys. Rev. A **22**, 1612 (1980).
[19] H. Bichsel, Rev. Mod. Phys. **60**, 663 (1988).
[20] C. C. Ahn, O. L. Krivanek, R. P. Burgner, M. M. Disko, and P. R. Swann, *EELS Atlas* (HREM Facility, Arizona State University, Tempe, AZ, 1983).
[21] H. Bichsel and N. Laulainen, Bull. Am. Phys. Soc. II **16**, 842 (1971). The paper describing this study has never been published. Stopping power, shell corrections, and I values were calculated.
[22] R. E. Johnson and M. Inokuti, Comments At. Mol. Phys. **14**, 19 (1983).
[23] ICRU, *Stopping Powers for Protons and Alpha Particles*, Report No. 48 (International Commission on Radiation Units and Measurements, Bethesda, MD, 1992).
[24] J. F. Bearden and A. F. Burr, Rev. Mod. Phys. **39**, 125 (1967).
[25] J. O. Hirschfelder and J. L. Magee, Phys. Rev. **73**, 207 (1948).
[26] G. S. Khandelwal, Nucl. Phys. A **116**, 97 (1968).
[27] E. Clementi, D. L. Raimondi, and W. P. Reinhardt, J. Chem. Phys. **47**, 1300 (1967).
[28] H. H. Andersen, J. F. Bak, H. Knudsen, and B. R. Nielsen, Phys. Rev. A **16**, 1929 (1977).
[29] G. Basbas, Nucl. Instrum. Methods B **4**, 227 (1984).
[30] H. Bichsel, Phys. Rev. A **41**, 3642 (1990).
[31] R. Medenwaldt, S. P. Møller, E. Uggerhøj, T. Worm, P. Hvelplund, H. Knudsen, K. Elsener, and E. Morenzoni, Phys. Lett. **155**, 155 (1991).
[32] *Handbook of Mathematical Functions*, Natl. Bur. Stand.

Appl. Math. Ser. No. 55, edited by M. Abramowitz and I. A. Stegun (U.S. GPO, Washington, DC, 1970)
[33] S. P. Ahlen, Phys. Rev. A **17**, 1236 (1978).
[34] S. P. Ahlen, Rev. Mod. Phys. **52**, 121 (1980).
[35] R. M. Sternheimer, S. T. Seltzer, and M. J. Berger, Phys. Rev. B **26**, 6067 (1982); At. Data Nucl. Data Tables **30**, 261 (1984).
[36] H. Bichsel and E. A. Uehling, Phys. Rev. **119**, 1670 (1960).
[37] H. Bichsel, Phys. Rev. **120**, 1012 (1960).
[38] M. J. Berger and S. Seltzer, in *Studies in Penetration of Charged Particles in Matter* (Ref. [13]), p. 69.
[39] H. Bichsel and T. Hiraoka, Int. J. Quantum. Chem. **23**, 565 (1989).
[40] D. Semrad (private communication).
[41] J. C. Oberlin, A. Amokrane, H. Beaumevieille, Y. Le Chalony, R. Perrier de la Bathie, and J. P. Stoquert, Radiat. Eff. **46**, 249 (1980).
[42] J. C. Oberlin, A. Amokrane, H. Beaumevieille, J. P. Stoquert, and R. Perrier de la Bathie, J. Phys. (Paris) **43**, 485 (1982).
[43] S. Matteson, J. M. Harris, R. Pretorius, and M-A. Nicolet, Nucl. Instrum. Methods **149**, 163 (1978).
[44] M. Luomajärvi, Radiat. Eff. **40**, 173 (1979).
[45] H. H. Andersen and B. R. Nielsen, Nucl. Instrum. Methods **191**, 475 (1981).
[46] D. C. Santry and R. D. Werner, Nucl. Instrum. Methods **185**, 517 (1981); **188**, 211 (1981).
[47] D. C. Santry and R. D. Werner, Nucl. Instrum. Methods B **1**, 13 (1984).
[48] R. Ishiwari, N. Shiomi, and N. Sakamoto, Nucl. Instrum. Methods B **2**, 141 (1984); **2**, 195 (1984).
[49] N. Shiomi, N. Sakamoto, K. Shima, T. Ishihara, K. Michikawa, S. Nagai, and R. Ishiwari, Nucl. Instrum. Methods B **13**, 107 (1986).
[50] H. Sørensen and H. H. Andersen, Phys. Rev. B **8**, 1854 (1973).
[51] M. Bader, R. E. Pixley, F. S. Mozer, and W. Whaling, Phys. Rev. **103**, 32 (1956).
[52] J. A. Borders, Radiat. Eff. **21**, 165 (1974).
[53] R. A. Langley and R. S. Blewer, Nucl. Instrum. Methods **132**, 109 (1976).
[54] D. W. Green, J. N. Cooper, and J. C. Harris, Phys. Rev. **98**, 466 (1955).
[55] H. Knudsen, H. H. Andersen, and V. Martini, Nucl. Instrum. Methods **168**, 41 (1980).
[56] V. Ya. Chumanov, Phys. Status Solidi A **53**, 51 (1979).
[57] R. Ishiwari, N. Shiomi-Tsuda, and N. Sakamoto, Nucl. Instrum. Methods B **31**, 503 (1988).
[58] N. Sakamoto, N. Shiomi, H. Ogawa, and R. Ishiwari, Nucl. Instrum. Methods B **13**, 115 (1986).
[59] J. G. Teasdale, University of California–Los Angeles Technical Report No. 3, 1949 (unpublished).
[60] C. P. Sonett and K. R. MacKenzie, Phys. Rev. **100**, 734 (1955).
[61] V. C. Burkig and K. R. MacKenzie, Phys. Rev. **106**, 848 (1957).
[62] G. H. Nakano, K. R. MacKenzie, and H. Bichsel, Phys. Rev. **132**, 291 (1963).
[63] W. K. Lin, H. G. Olson, and D. Powers, Phys. Rev. B **8**, 1881 (1973).
[64] W. K. Lin, S. Matteson, and D. Powers, Phys. Rev. B **10**, 3746 (1974).
[65] H. H. Andersen, C. C. Hanke, H. Sørensen, and P. Vajda, Phys. Rev. **153**, 338 (1967).
[66] H. H. Andersen, H. Simonsen, H. Sørensen, and P. Vajda, Phys. Rev. **186**, 372 (1969).
[67] A. Fontell and M. Luomajärvi, Phys. Rev. B **19**, 159 (1979).
[68] W. K. Chu, J. F. Ziegler, I. V. Mitchell, and W. D. Mackintosh, Appl. Phys. Lett. **22**, 437 (1973).
[69] E. I. Sirotinin, A. F. Tulinov, V. A. Khodyrev, and V. N. Mizgulin, Nucl. Instrum. Methods B **4**, 337 (1984).
[70] Kuldeep and A. K. Jain, Nucl. Instrum. Methods B **9**, 259 (1985).
[71] H. Bichsel, National Institute of Standards and Technology Report No. NISTIR 4550, 1991 (unpublished).
[72] N. Sakamoto, H. Ogawa, M. Mannami, K. Kimura, Y. Susuki, M. Hasegawa, I. Katayama, T. Noro, and H. Ikegami, Radiat. Eff. Def. Solids **117**, 193 (1991).
[73] C. J. Bakker and E. Segrè, Phys. Rev. **81**, 489 (1951).
[74] W. H. Barkas and S. von Friesen, Nuovo Cimento Suppl. **19**, 41 (1961).
[75] I. M. Vasilevsky and Yu. D. Prokoshkin, Yad. Fiz. **4**, 549 (1966) [Sov. J. Nucl. Phys. **4**, 390 (1967)].
[76] I. M. Vasilevsky, I. I. Karpov, V. I. Petrushkin, and Yu. D. Prokoshkin, Yad. Fiz. **9**, 997 (1969) [Sov. J. Nucl. Phys. **9**, 583 (1969)].
[77] R. Ishiwari, N. Shiomi, S. Shirai, T. Ohata, and Y. Uemura, Bull. Inst. Chem. Res., Kyoto Univ. **49**, 403 (1971).
[78] R. Ishiwari, N. Shiomi, T. Kinoshita, and F. Yasue, Bull. Inst. Chem. Res., Kyoto Univ. **55**, 68 (1977).
[79] R. Ishiwari, N. Shiomi, and N. Sakamoto, Bull. Inst. Chem. Res., Kyoto Univ. **56**, 47 (1978).
[80] T. Takahashi, Y. Awaya, T. Tonuma, H. Kumagai, K. Izumo, M. Nishida, A. Hitachi, A. Hashizume, S. Uchiyama, and T. Doke, Phys. Rev. A **27**, 1360 (1983).
[81] R. Bimbot, S. Della Negra, D. Gardes, H. Gauvin, A. Fleury, and F. Hubert, Nucl. Instrum. Methods **153**, 161 (1978).
[82] R. Bimbot, H. Gauvin, I. Orliange, R. Anne, G. Bastin, and F. Hubert, Nucl. Instrum. Methods B **17**, 1 (1986).
[83] H. Gauvin and R. F. Hubert, Nucl. Instrum. Methods B **28**, 191 (1987).
[84] Th. Schwab, H. Geissel, P. Armbruster, A. Gillibert, W. Mittig, R. E. Olson, K. B. Winterbon, H. Wollnik, and G. Münzenberg, Gesellschaft für Schwerionenforschung Report No. GSI-89-79, 1989 (unpublished).
[85] H. Bichsel, R. F. Mozley, and W. A. Aron, Phys. Rev. **105**, 1788 (1957).
[86] H. W. Lewis, Phys. Rev. **85**, 20 (1952).
[87] N. Bloembergen and P. J. van Heerden, Phys. Rev. **83**, 561 (1951).
[88] R. Mather and E. Segrè, Phys. Rev. **84**, 191 (1951).
[89] C. F. Williamson, J.-P. Boujot, and J. Picard, Centre d'Etudes Nucléaires de Saclay Report No. CEA-R 3042 1966 (unpublished).
[90] A. Arnau, M. Peñalba, P. M. Echenique, F. Flores, and R. H. Ritchie, Phys. Rev. Lett. **65**, 1024 (1990).
[91] R. Anholt, Phys. Rev. A **19**, 1004 (1979).
[92] D. D. Cohen and M. Harrigan, At. Data Nucl. Data Tables **33**, 255 (1985).
[93] M. Pajek *et al.*, Phys. Rev. A **42**, 261 (1990).
[94] P. T. Leung, Phys. Rev. A **40**, 5417 (1989).
[95] M. L. Rustgi, P. T. Leung, and S. A. T. Long, Phys. Rev. A **37**, 1775 (1988).